Monogamy relations within quadripartite Einstein-Podolsky-Rosen steering based on cascaded four-wave mixing processes

Yu Xiang,[1,2,3] Yang Liu,[4,5,6] Yin Cai,[4,*] Feng Li,[4] Yanpeng Zhang,[4] and Qiongyi He[1,2,3]

[1]*State Key Laboratory of Mesoscopic Physics, School of Physics, Nano-optoelectronics Frontier Center of the Ministry of Education and Collaborative Innovation Center of Quantum Matter, Peking University, Beijing 100871, China*

[2]*Beijing Academy of Quantum Information Sciences, Beijing 100193, China*

[3]*Collaborative Innovation Center of Extreme Optics, Shanxi University, Taiyuan, Shanxi 030006, China*

[4]*Key Laboratory for Physical Electronics and Devices of the Ministry of Education and Shaanxi Key Lab of Information Photonic Technique, Xi'an Jiaotong University, Xi'an 710049, China*

[5]*State Key Laboratory of Transient Optics and Photonics, Xi'an Institute of Optics and Precision Mechanics, Chinese Academy of Sciences, Xi'an 710119, China*

[6]*University of Chinese Academy of Sciences, Beijing 100049, China*

(Received 31 December 2019; accepted 28 April 2020; published 15 May 2020)

Multipartite Einstein-Podolsky-Rosen (EPR) steering has been recognized as an essential resource for secure quantum communication tasks composed of several spatially separated parties who cannot be fully trusted. Nevertheless, this resource cannot be distributed arbitrarily over many parties; for instance, two independent players cannot simultaneously steer the third party by two-setting measurements. This feature is referred to as monogamy of steering, which ensures the security of quantum cryptographic protocols and is thus a very desired property to investigate for multipartite steering. Here, we propose symmetric and asymmetric structures of cascaded four-wave mixing of rubidium atoms to generate versatile quadripartite EPR steering and investigate four distinct types of monogamy relations of Gaussian steering. We find that the distribution constraint described by one of the monogamy relations can be lifted only for the quadripartite steering created by the symmetric setup. This result paves the way for a better understanding of the distribution rules of multipartite EPR steering and its potential applications for secure quantum communication.

DOI: 10.1103/PhysRevA.101.053834

I. INTRODUCTION

Schrödinger first introduced the term "steering" [1] to describe the "spooky action-at-a-distance" phenomenon indicated in the famous Einstein-Podolsky-Rosen (EPR) paradox in 1935 [2]. To test this paradox for continuous-variable systems, Reid introduced an experimental criterion based on the inferred Heisenberg uncertainty relation [3]. Later on, the concept of steering was formalized mathematically for mixed states through an asymmetric model called the local-hidden-state (LHS) model [4]. The authors pointed out that steering is an intermediate type of quantum correlations between state inseparability and Bell nonlocality from the quantum information perspective; that is, EPR steering allows one to verify entanglement shared between Alice and Bob without the assumptions of the full trust of their devices [5,6]. Due to this inherent asymmetric quantum property [7–12], EPR steering has been recognized as an essential resource for one-sided device-independent (1sDI) quantum cryptography tasks [13–20], which is an asymmetric scenario between DI quantum cryptography based on states that give violations of a Bell inequality and device-dependent protocols (where both sites are trusted) relying on inseparable quantum states.

Motivated by the demand for constructing large-scale entangled states for a quantum network, EPR steering has been extended to multipartite scenarios [21–26]. Recently, continuous-variable multipartite EPR steering of up to four and eight modes was achieved by linear optics networks composed of squeezed and vacuum modes mixed by beam splitters [27,28], and even more, that to 16 modes was realized by the optical frequency comb system [29]. Another powerful method is applying single-pass four-wave mixing (FWM) based on Rb vapors to generate squeezed lights [30] and multipartite entanglement [31,32]. Recently, Jing's group made significant advances in developing multimode entanglement by a cascaded regime and generated spatially multiple quantum modes with strong correlations [33–36]. This method provides a wide phase-matching range for spatial modes without the need for optical cavities or phase control [37,38]. Moreover, atomic media can be used to store the entangled photons with narrow bandwidth for quantum memory effectively [39–41]. In addition, the FWM process could also be applied for quantum information processing and quantum metrology, such as the tunable delay of EPR entangled states [42], a nonlinear interferometer with parametric amplifiers such as beam splitters [43–45], a controllable graph state [46], and the generation of high spectral brightness and purity narrow-band single photons [47]. Therefore, it is desirable to study how the quantum steering can be created and distributed

*caiyin@xjtu.edu.cn

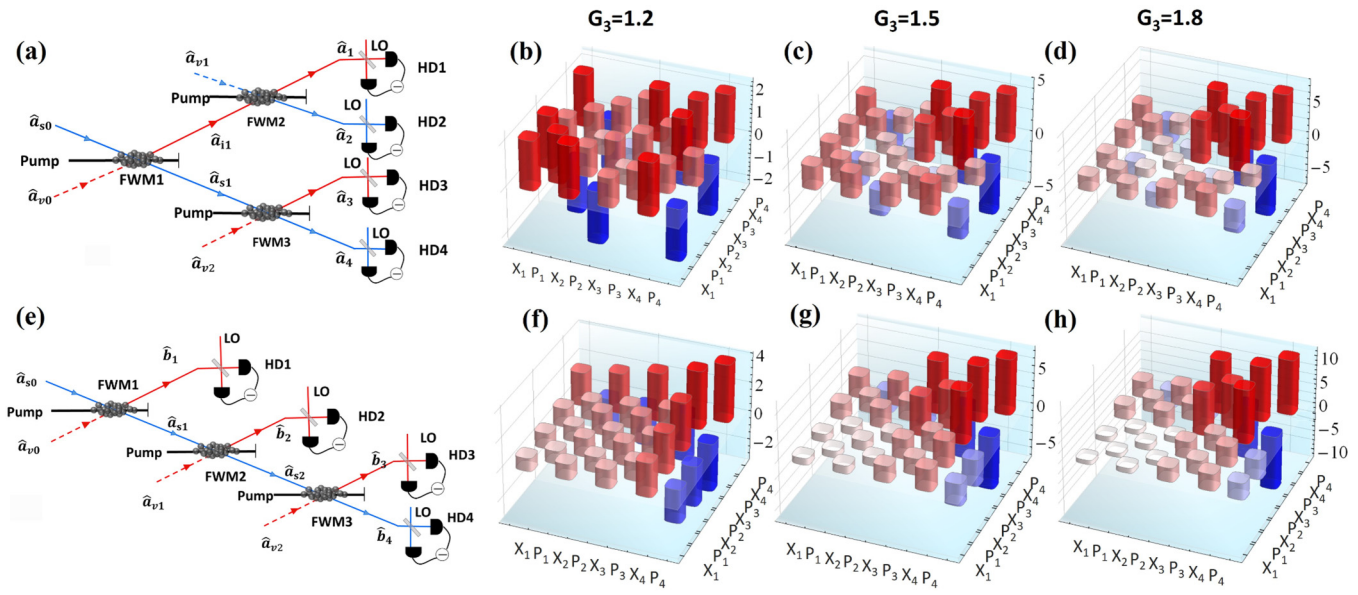

FIG. 1. (a) Schematic diagram of generating quadripartite entangled states using a symmetric structure of three cascaded FWM processes. $\hat{a}_{s_0}$ is the seed input; $\hat{a}_{v_0}$, $\hat{a}_{v_1}$ and $\hat{a}_{v_2}$ are the three vacuum modes; $\hat{a}_{i_1}$ and $\hat{a}_{s_1}$ are the output idler and signal beams of FWM1; and $\hat{a}_{1,2,3,4}$ are the final four output modes after FWM2 and FWM3. (b)–(d) Covariance matrices of the output four-mode Gaussian states with fixed gain factors $G_1 = G_2 = 1.2$ and variable $G_3 = 1.2,\ 1.5,\ 1.8$, respectively. (e) Schematic diagram of the asymmetric structure. (f)–(h) Covariance matrices of the output modes $\hat{b}_{1,2,3,4}$ with fixed $G_1 = G_2 = 1.2$ and variable $G_3 = 1.2,\ 1.5,\ 1.8$, respectively. LO denotes the local oscillator for homodyne detection techniques (HD1–HD4). To clearly visualize quantum correlations, the shot noises (which are unity) are subtracted from the diagonal terms of the CMs.

by the FWM process and to investigate the different properties of multipartite steering relying on the cascaded structures.

Here, we study the four-mode steering created by symmetric and asymmetric structures of three cascaded FWM processes, as shown in Fig. 1, and analyze the difference in steering properties created by two structures. By quantifying the steerability via a measure based on the symplectic eigenvalues of the covariance matrix (CM) [22], we study the various properties of EPR steering shared by two, three, four modes, which confirm four types of monogamy relations of Gaussian steering. Interestingly, we show that one specific monogamy constraint can be lifted only for the states generated by the symmetric structure of the cascaded FWM scheme. The characters and the distribution of steering among modes are determined by the structure of cascaded FWM processes; for example, the symmetric structure generates two idler and two signal outputs, while the asymmetric one generates three idler and one signal beams. Since entanglement can be shared only between idler and signal beams, the asymmetric setup sets more constraints for distributing steering. Moreover, using the Bloch-Messiah reduction [48,49], we transform the output four-mode Gaussian states into a set of uncorrelated eigenmodes and find that the states produced by the symmetric cascaded FWM processes are composed of more squeezed eigenmodes. These structural differences are helpful to gauge the availability of these states for different quantum communication tasks.

The remainder of this paper is organized as follows. In Sec. II, we present two structures of three cascaded FWM processes, the produced four-mode Gaussian states, and their CMs. In Sec. III, we recall the Gaussian steering measure adopted in this work and investigate the steering shared by two, three, and four modes and the corresponding monogamy relations. In Sec. IV, we analyze the essential physics of different steering properties created in two structures. Finally, we summarize in Sec. V.

II. THE GENERATION OF FOUR-MODE GAUSSIAN STATES

Within a FWM process, an intense pump beam and a weak seed beam are focused in the center of the Rb vapor cell with a slight angle. During a third-order optical nonlinear process, a signal beam is amplified, and an idler beam is generated simultaneously. In practice, the pump beam is tuned about 0.8 GHz to the blue of the D_1 line of Rb ($5S_{1/2}, F = 2 \rightarrow 5P_{1/2}$), and the seed beam is red tuned about 3 GHz to the pump beam. The two-photon detuning is about 4 MHz [33,50]. The energy conservation and phase-matching conditions must be satisfied in each FWM process whose input-output relation can be presented by

$$\hat{a}_{s_1} = G_1\hat{a}_{s_0} + g_1\hat{a}^{\dagger}_{v_0}, \quad \hat{a}_{i_i} = g_1\hat{a}^{\dagger}_{s_0} + G_1\hat{a}_{v_0}, \tag{1}$$

where G_1 is the amplitude gain in the FWM1 process and $g_1 = \sqrt{G_1^2 - 1}$, $\hat{a}^{\dagger}_{s(v)_0}$ and $\hat{a}_{s(v)_0}$ are the creation and annihilation operators of the seed (vacuum) input, and $\hat{a}_{s_1}$ and $\hat{a}_{i_1}$ are the annihilation operators of the output signal and idler beams, respectively. As shown in Figs. 1(a) and 1(e), two cascaded networks are constructed by three FWM processes with symmetric and asymmetric structures, respectively. The FWM2 and FWM3 processes have the same input-output relations. In the symmetric case, the output signal beam $\hat{a}_{s_1}$ and idler beam $\hat{a}_{i_1}$ of the first cell are used to seed FWM2 and FWM3, respectively; however, in the asymmetric structure, only the output signal beam $\hat{a}_{s_1}$ is used to seed FWM2, and the signal

beam $\hat{a}_{s2}$ generated by FWM2 is to further seed FWM3. Based on the cascaded FWM processes introduced above, two types of four-mode Gaussian states $\hat{a}_{1,2,3,4}$ and $\hat{b}_{1,2,3,4}$ are generated.

The correlation properties of four-mode Gaussian states are fully given by their CMs. The amplitude and phase quadrature operators are defined as $\hat{X} = \hat{a} + \hat{a}^\dagger$ and $\hat{P} = i(\hat{a}^\dagger - \hat{a})$, respectively. The input-output relations of symmetric and asymmetric structures are written as $\vec{\xi}_{\rm sym} = U_{\rm sym}\vec{\xi}_{\rm in}$ and $\vec{\xi}_{\rm asy} = U_{\rm asy}\vec{\xi}_{\rm in}$, respectively, where $\vec{\xi}_{\rm sym} = (\hat{X}_1^a, \hat{P}_1^a, \hat{X}_2^a, \hat{P}_2^a, \hat{X}_3^a, \hat{P}_3^a, \hat{X}_4^a, \hat{P}_4^a)^\top$, $\vec{\xi}_{\rm asy} = (\hat{X}_1^b, \hat{P}_1^b, X_2^b, \hat{P}_2^b, \hat{X}_3^b, \hat{P}_3^b, \hat{X}_4^b, \hat{P}_4^b)^\top$, and $\vec{\xi}_{\rm in} = (\hat{X}_{s_0}, \hat{P}_{s_0}, \hat{X}_{v_0}, \hat{P}_{v_0}, \hat{X}_{v_1}, \hat{P}_{v_1}, \hat{X}_{v_2}, \hat{P}_{v_2})^\top$. The transform operation matrices $U_{\rm sym}$ and $U_{\rm asy}$ are written as

$$U_{\rm sym} = \begin{pmatrix} g_1G_2 & 0 & G_1G_2 & 0 & g_2 & 0 & 0 & 0 \\ 0 & -g_1G_2 & 0 & G_1G_2 & 0 & -g_2 & 0 & 0 \\ g_1g_2 & 0 & G_1g_2 & 0 & G_2 & 0 & 0 & 0 \\ 0 & g_1g_2 & 0 & -G_1g_2 & 0 & G_2 & 0 & 0 \\ G_1g_3 & 0 & g_1g_3 & 0 & 0 & 0 & G_3 & 0 \\ 0 & -G_1g_3 & 0 & g_1g_3 & 0 & 0 & 0 & G_3 \\ G_1G_3 & 0 & g_1G_3 & 0 & 0 & 0 & g_3 & 0 \\ 0 & G_1G_3 & 0 & -g_1G_3 & 0 & 0 & 0 & -g_3 \end{pmatrix}, \tag{2a}$$

$$U_{\rm asy} = \begin{pmatrix} g_1 & 0 & G_1 & 0 & 0 & 0 & 0 & 0 \\ 0 & -g_1 & 0 & G_1 & 0 & 0 & 0 & 0 \\ G_1g_2 & 0 & g_1g_2 & 0 & G_2 & 0 & 0 & 0 \\ 0 & -G_1g_2 & 0 & g_1g_2 & 0 & G_2 & 0 & 0 \\ G_1G_2g_3 & 0 & g_1G_2g_3 & 0 & g_2g_3 & 0 & G_3 & 0 \\ 0 & -G_1G_2g_3 & 0 & g_1G_2g_3 & 0 & g_2g_3 & 0 & G_3 \\ G_1G_2G_3 & 0 & g_1G_2G_3 & 0 & g_2G_3 & 0 & g_3 & 0 \\ 0 & G_1G_2G_3 & 0 & -g_1G_2G_3 & 0 & -g_2G_3 & 0 & -g_3 \end{pmatrix}. \tag{2b}$$

The elements of the CM of Gaussian states are defined as $C_{ij} = \langle\vec{\xi}_i\vec{\xi}_j + \vec{\xi}_j\vec{\xi}_i\rangle/2 - \langle\vec{\xi}_i\rangle\langle\vec{\xi}_j\rangle$. The CMs with fixed $G_1 = G_2 = 1.2$ and variable $G_3 = 1.2$, 1.5, 1.8 for symmetric and asymmetric structures are presented in Figs. 1(b)–1(d) and 1(f)–1(h), respectively. By adjusting the gain parameters in two structures, one can modulate quantum correlations shared among four output modes. Note that there are no cross correlations between the amplitude and phase quadratures, so the corresponding terms in CMs are all zero.

III. THE PROPERTIES OF EPR STEERING

Based on the CMs of the produced four-mode Gaussian states, we are ready to quantify the EPR steering shared among modes in two different structures. The CM of any bipartition Gaussian state containing $(n_{\mathcal{A}} + n_{\mathcal{B}})$ modes can be written as $\sigma_{AB} = \left(\begin{smallmatrix} \mathcal{A} & C \\ C^\top & \mathcal{B} \end{smallmatrix}\right)$, where submatrices $\mathcal{A}$ and $\mathcal{B}$ are CMs of the reduced state of their respective subsystems. Then, the steerability from subsystem A to subsystem B can be quantified by [22]

$$\mathcal{G}^{A\to B}(\sigma_{AB}) = \max\left\{0, -\sum_{j:\bar{\nu}_j^{\mathcal{AB}/\mathcal{A}}<1} \ln\left(\bar{\nu}_j^{\mathcal{AB}/\mathcal{A}}\right)\right\}, \tag{3}$$

where $\bar{\nu}_j^{\mathcal{AB}/\mathcal{A}} (j = 1, \ldots, n_{\mathcal{B}})$ are the symplectic eigenvalues of $\bar{\sigma}_{\mathcal{AB}/\mathcal{A}} = \mathcal{B} - C^T\mathcal{A}^{-1}C$, derived from the Schur complement of $\mathcal{A}$ in the covariance matrix σ_{AB}. Note that the criterion of $\mathcal{G}^{A\to B} > 0$ is a sufficient and necessary condition for testing steering of Gaussian states with quadrature measurements. In a non-Gaussian scenario (either non-Gaussian states or non-Gaussian measurements or both), this criterion still validates the presence of steering, but it is not a necessary condition [51].

A. The (1 + 1)-mode EPR steering and type-I monogamy relation

We start with the investigation of $(1 + 1)$-mode EPR steering. From the analytical solutions given in Appendix 1 and 2, we find that there is no steering between modes $\hat{a}_1$ and $\hat{a}_3$, $\hat{a}_2$ and $\hat{a}_4$, and among modes $\hat{b}_1$, $\hat{b}_2$, and $\hat{b}_3$ for the states generated by the symmetric and asymmetric structures, respectively. Moreover, in both cases the asymmetric steering is observed where the steering in one direction always exists but the presence of steering in the other direction is conditional on the values of gain factors [10–12]. This is illustrated in Figs. 2(a)–2(d), where $\mathcal{G}^{a_4\to a_3} > 0$ ($\mathcal{G}^{b_4\to b_3} > 0$) for all $G_3 > 1.0$, while $\mathcal{G}^{a_3\to a_4} > 0$ ($\mathcal{G}^{b_3\to b_4} > 0$) only when $G_3 > 1.14$ ($G_3 > 1.23$ and $G_3 > 1.35$ for the cases of $G_2 = 1.2$ and $G_2 = 2.0$, respectively). Note that the value of G_2 does not affect the steerability between modes a_4 and a_3 in the symmetric FWM processes but does affect the steerability between modes b_4 and b_3 in the asymmetric case. All those characters are well understood from the analysis of the roles of output beams after FWM and the asymmetrical effect of thermal noises on the steered and steering parties in Sec. IV.

We can see that in two cases neither $\hat{a}_4$ nor $\hat{b}_4$ can be steered by more than one mode simultaneously. This agrees with the type-I monogamy relation for Gaussian steering introduced by Reid [52] in which two distinct modes cannot steer the

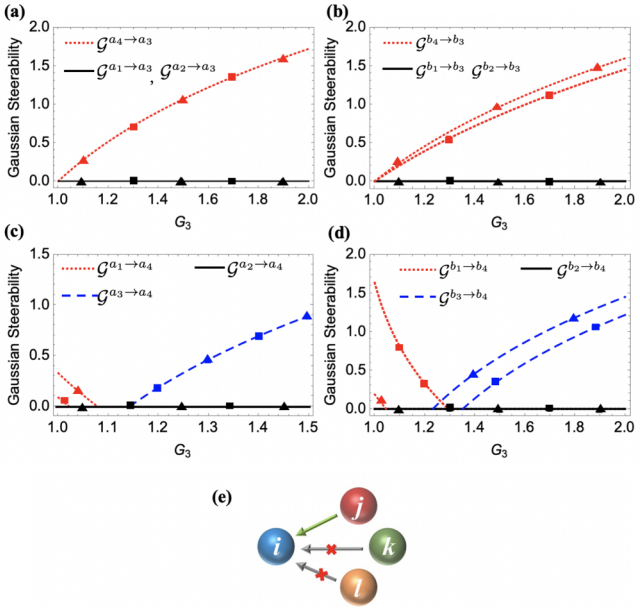

FIG. 2. The $(1+1)$-mode steering varying with G_3 for fixed gain values $G_1 = 1.2$, $G_2 = 1.2$ (lines with triangles), or 2 (lines with squares). (a) Mode $\hat{a}_4$ can always steer $\hat{a}_3$, and its steerability $\mathcal{G}^{a_4\to a_3}$ grows with increasing G_3, while neither $\hat{a}_1$ nor $\hat{a}_2$ can steer $\hat{a}_3$. (b) Mode $\hat{b}_4$ can always steer $\hat{b}_3$, and $\mathcal{G}^{b_4\to b_3}$ increases with G_3 and also depends on the value of G_2. Meanwhile, neither $\hat{b}_1$ nor $\hat{b}_2$ can steer $\hat{b}_3$. (c) Mode $\hat{a}_4$ can be steered by mode $\hat{a}_1$ or $\hat{a}_3$ conditionally. G_2 has influence on the steerability of $\mathcal{G}^{a_1\to a_4}$ but not on $\mathcal{G}^{a_3\to a_4}$. (d) Mode $\hat{b}_4$ can be steered by mode $\hat{b}_2$ or $\hat{b}_3$ conditionally, and their steerabilities are affected by the value of G_2. The above results validate the type-I monogamy relation described in (e).

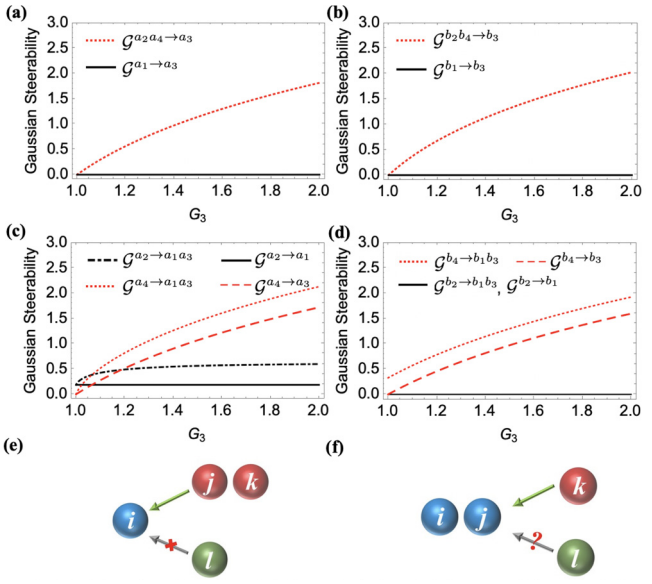

FIG. 3. The $(1+2)$- and $(2+1)$-mode steerings with fixed gain values $G_1 = G_2 = 1.2$ and variable values of G_3. (a) Mode $\hat{a}_3$ can be steered by modes $(\hat{a}_2\hat{a}_4)$ jointly but cannot be steered by $\hat{a}_1$. (b) Mode $\hat{b}_3$ can be steered by modes $(\hat{b}_2\hat{b}_4)$ jointly but cannot be steered by $\hat{b}_1$. (c) Modes $(\hat{a}_1\hat{a}_3)$ can be steered by modes $\hat{a}_2$ and $\hat{a}_4$ simultaneously. (d) Modes $(\hat{b}_1\hat{b}_3)$ can be steered by $\hat{b}_4$ but cannot be steered by $\hat{b}_2$ simultaneously. The simplified schematic of the type-II monogamy relation for which (e) the steering party contains more than one mode and (f) the steered party contains two modes. Note that the constraint sketched in (f) may be lifted for the states created by the symmetric cascaded FWM processes as presented in (c).

third mode simultaneously with Gaussian measurements. In our four-mode case, this means $\mathcal{G}^{j\to i} > 0 \Rightarrow \mathcal{G}^{k\to i} = \mathcal{G}^{l\to i} = 0$, where i, j, k, l represent the four modes in two structures, as sketched in Fig. 2(e).

B. The (1 + 2)- and (2 + 1)-mode steering and type-II monogamy relation

Now we move to investigate $(1+2)$- and $(2+1)$-mode steering where either the steered party or steering party contains two modes. Since the general analytical solutions do not have simple forms, we only give some of them for asymmetric structure in Appendix 3. Figure 3(a) shows that the group $(\hat{a}_2\hat{a}_4)$ can always steer mode $\hat{a}_3$, while the remaining mode $\hat{a}_1$ cannot steer mode $\hat{a}_3$ simultaneously. A similar observation for the asymmetric structure is depicted in Fig. 3(b). This agrees with a generalized form of the type-I monogamy relation; that is, two independent groups of modes cannot simultaneously steer the third single mode with Gaussian measurements [53,54]. In our four-mode case, this means $\mathcal{G}^{jk\to i} > 0 \Rightarrow \mathcal{G}^{l\to i} = 0$, referred to as the type-II monogamy relation, illustrated by Fig. 3(e).

Interestingly, when the steered party contains more than one mode, we find that the steerabilities $\mathcal{G}^{a_2\to(a_1a_3)} > 0$ and $\mathcal{G}^{a_4\to(a_1a_3)} > 0$ occur simultaneously, as shown in Fig. 3(c) for the symmetric structure, which means the type-II monogamy constraint can be lifted when more than one mode is steered, i.e., $\mathcal{G}^{k\to ij} > 0 \not\Rightarrow \mathcal{G}^{l\to ij} = 0$, as sketched in Fig. 3(f). However, this lift cannot be observed in the asymmetric structure, as shown in Fig. 3(d), where $\mathcal{G}^{b_4\to(b_1b_3)} > 0$ and $\mathcal{G}^{b_2\to(b_1b_3)} = 0$. The explanation will follow from the eigensqueezers coexisting in the system detailed in Sec. IV.

C. The (1 + 3)- and (3 + 1)-mode steering and type-III monogamy

In this part we quantify how the EPR steering is distributed among four modes. Figure 4(a) shows the joint steering of mode $\hat{a}_4$ by the left three modes together and by each individual mode. It is seen that with fixed $G_1 = G_2 = 1.2$, $\mathcal{G}^{a_1a_2a_3\to a_4} > 0$ for any value of $G_3 > 1$, but $\mathcal{G}^{a_1\to a_4} > 0$ and $\mathcal{G}^{a_3\to a_4} > 0$ at $G_3 \in (1, 1.08)$ and $G_3 > 1.14$, respectively, and $\mathcal{G}^{a_2\to a_4} = 0$ all the time. Although the individual modes $\hat{a}_1$, $\hat{a}_2$, $\hat{a}_3$ cannot steer $\hat{a}_4$ simultaneously, constrained by the type-I monogamy, the steerability by them together is significantly enhanced. Similar phenomena are observed for the asymmetric structure shown in Fig. 4(b), with even stronger joint steerability $\mathcal{G}^{b_1b_2b_3\to b_4} > \mathcal{G}^{a_1a_2a_3\to a_4}$. This is because by cascading more FWM processes in the asymmetric structure one can generate lager squeezing values in the system, as discussed in Sec. IV.

In both cases, the enhanced joint steerability is even stronger than the sum of the pairwise steerability, i.e., $\mathcal{G}^{a_1a_2a_3\to a_4} - \sum_{n=1}^{3}\mathcal{G}^{a_n\to a_4} > 0$ and $\mathcal{G}^{b_1b_2b_3\to b_4} - \sum_{n=1}^{3}\mathcal{G}^{b_n\to b_4} > 0$, as indicated in Figs. 4(c) and 4(d).

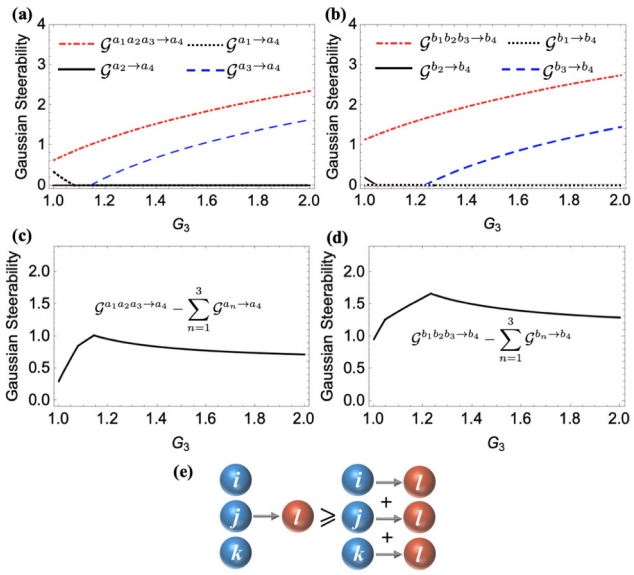

FIG. 4. The $(3+1)$-mode steering varying with G_3 for fixed gain values $G_1 = G_2 = 1.2$. (a) Modes $(\hat{a}_1\hat{a}_2\hat{a}_3)$ jointly steer $\hat{a}_4$, and mode $\hat{a}_1$ or $\hat{a}_3$ can individually steer $\hat{a}_4$ with different G_3. (b) Modes $(\hat{b}_1\hat{b}_2\hat{b}_3)$ jointly steer $\hat{b}_4$, and individual mode $\hat{b}_2$ or $\hat{b}_3$ can conditionally steer $\hat{b}_4$ with different G_3. The residual Gaussian steering for (c) the symmetric structure and (d) asymmetric case, which stem from the type-III monogamy relation indicated in (e).

This is also true for the opposite direction, i.e., $\mathcal{G}^{a_4\to a_1a_2a_3} - \sum_{n=1}^{3}\mathcal{G}^{a_4\to a_n} > 0$ and $\mathcal{G}^{b_4\to b_1b_2b_3} - \sum_{n=1}^{3}\mathcal{G}^{b_4\to b_n} > 0$, as plotted in Figs. 5(c) and 5(d). In fact, this observation meets the constraint introduced by the type-III monogamy relation,

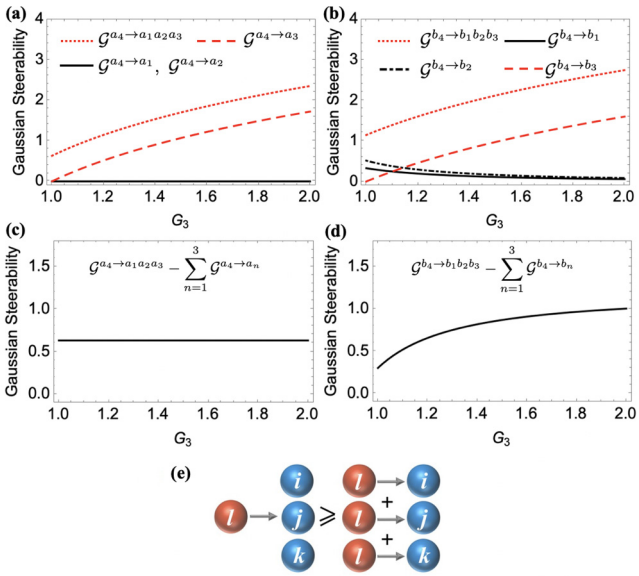

FIG. 5. The $(1+3)$-mode steering varying with G_3 for fixed gain values $G_1 = G_2 = 1.2$. (a) The steering from mode $\hat{a}_4$ to individual $\hat{a}_1$, $\hat{a}_2$, $\hat{a}_3$ and the group of them. (b) The steering from mode $\hat{b}_4$ to individual $\hat{b}_1$, $\hat{b}_2$, $\hat{b}_3$ and the group of them. The residual Gaussian steering for (c) the symmetric structure and (d) asymmetric case, which stem from the type-III monogamy relation indicated in (e).

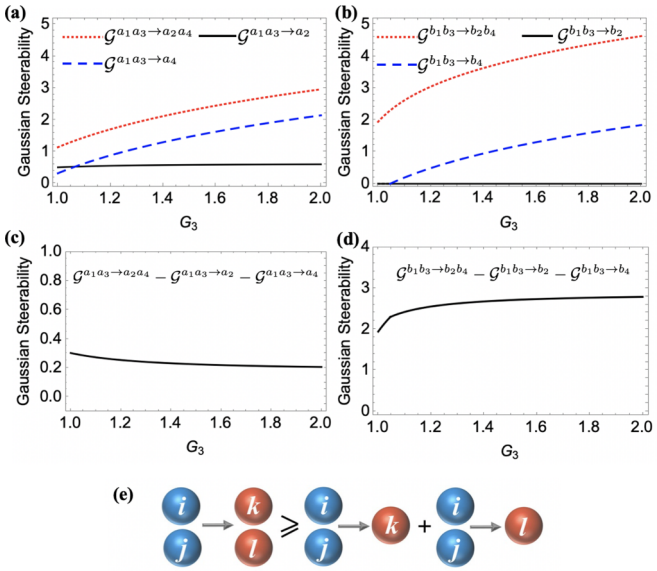

FIG. 6. The $(2+2)$-mode and corresponding $(2+1)$-mode steerings varying with G_3 for fixed gain values $G_1 = G_2 = 1.2$. (a) Modes $(\hat{a}_1\hat{a}_3)$ jointly steer $\hat{a}_2$, $\hat{a}_4$ and the group of them, respectively. (b) Modes $(\hat{b}_1\hat{b}_3)$ jointly steer $\hat{b}_2$, $\hat{b}_4$ and the group of them, respectively. The difference between $(2+2)$-mode steerability and the sum of $(2+1)$-mode steerability in (c) the symmetric structure and in (d) the asymmetric case. (e) The simplified schematic of type-IV monogamy relation (5a).

named Coffman-Kundu-Wootters-type monogamy [24]. For the four-mode scenario, it reads

$$\mathcal{G}^{ijk\to l} - \mathcal{G}^{i\to l} - \mathcal{G}^{j\to l} - \mathcal{G}^{k\to l} \geqslant 0, \tag{4a}$$

$$\mathcal{G}^{l\to ijk} - \mathcal{G}^{l\to i} - \mathcal{G}^{l\to j} - \mathcal{G}^{l\to k} \geqslant 0, \tag{4b}$$

which are valid for all Gaussian states with Gaussian measurements.

Note that for the state created by the symmetric case mode $\hat{a}_4$ cannot steer the individual modes $\hat{a}_1, \hat{a}_2, \hat{a}_3$ simultaneously, as shown in Fig. 5(a), while for the asymmetric case mode $\hat{b}_4$ can always steer the individual modes $\hat{b}_1$, $\hat{b}_2$, $\hat{b}_3$ at the same time when $G_3 > 1.0$, as shown in Fig. 5(b). This can be understood following the analysis of the difference in the two structures in Sec. IV.

D. The (2 + 2)-mode steering and type-IV monogamy relation

Finally, we study a more general type of steering properties where both the steering party and the steered party contain more than one mode. We select one example with respect to the bipartition (1,3)-(2,4). The steerings in the directions $(1,3)\to(2,4)$, $(1,3)\to(2)$, and $(1,3)\to(4)$ are shown in Figs. 6(a) and 6(b) for the symmetric and asymmetric cases, respectively. Figures 6(c) and 6(d) show that the $(2+2)$-mode steerability is stronger than the sum of the $(2+1)$-mode steerability. Analogously, we get the same result in Fig. 7, where the $(2+2)$-mode steerability is stronger than the sum of the $(1+2)$-mode steerability. This confirms a more general

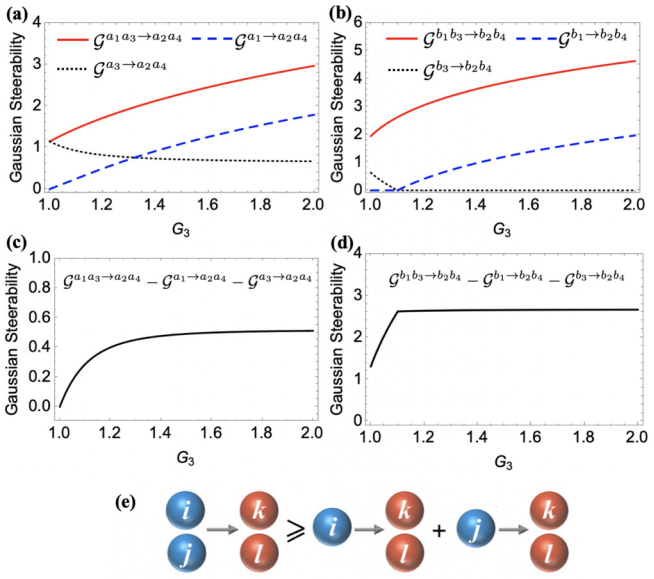

FIG. 7. The $(2+2)$-mode and corresponding $(1+2)$-mode steerings varying with G_3 for fixed gain values $G_1 = G_2 = 1.2$. (a) Modes $(\hat{a}_2\hat{a}_4)$ are steered by $\hat{a}_1$, $\hat{a}_3$ and their collaboration. (c) Modes $(\hat{b}_2\hat{b}_4)$ are steered by $\hat{b}_1$, $\hat{b}_3$ and their collaboration. The difference between $(2+2)$-mode steerability and the sum of $(1+2)$-mode steerability in the (c) symmetric structure and in (d) the asymmetric case. (e) The simplified schematic of type-IV monogamy relation (5b).

version of the type-III monogamy relation for Gaussian steerability [55], which is written as for our four-mode scenario,

$$\mathcal{G}^{ij\to kl} - \mathcal{G}^{ij\to k} - \mathcal{G}^{ij\to l} \geqslant 0, \tag{5a}$$

$$\mathcal{G}^{ij\to kl} - \mathcal{G}^{i\to kl} - \mathcal{G}^{j\to ikl} \geqslant 0, \tag{5b}$$

sketched in Figs. 6(e) and 7(e). Note that the constraint described by Eq. (5b) can be lifted when the system is not pure [55]. The present states created by two cascaded FWM structures are pure such that the type-IV monogamy relation is valid for all possible $(2+2)$-mode configurations.

Note that the lifting of the type-II constraint is also observed in Fig. 7(a) where the group $(\hat{a}_2\hat{a}_4)$ can be steered by mode $\hat{a}_1$ and by mode $\hat{a}_3$ simultaneously.

IV. DISCUSSION

In order to understand the essential physics of the above steering properties, in particular, why the lifting of the constraint given by the type-II monogamy relation can be observed only for the states created by the cascaded FWM processes in a symmetric structure, in this section we analyze the difference in the two structures and the squeezed eigenmodes decomposed from four-mode Gaussian states.

A. The difference in steering properties created by two cascaded FWM structures

The characteristics of all the pairwise quantum steerings created by the two structures are discussed here in detail, as they underlie the properties of quantum steering shared by more modes. Based on the solutions given in Appendix 1 and

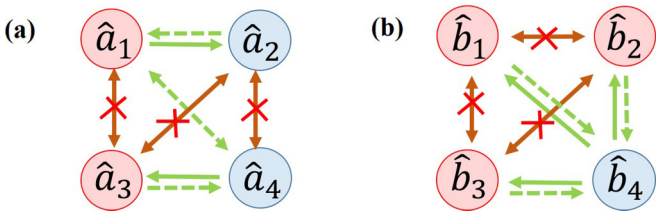

FIG. 8. All pairwise EPR steerings for (a) the symmetric structure and (b) asymmetric structure. The red and blue circles represent the signal and idler beams plotted in Figs. 1(a) and 1(e), respectively. Solid red lines with a cross, solid green lines, and dashed green lines represent no steering, deterministic steering, and conditional steering, respectively.

2, we plot in Fig. 8 all possible $(1+1)$-mode steerings in both structures corresponding to the parameters used in Figs. 2–7. It is clear that the four-mode Gaussian states produced by the two structures possess different steering properties. First, there is no pairwise steering between $\hat{a}_1$ and $\hat{a}_3$, $\hat{a}_2$ and $\hat{a}_4$, and no pairwise steering among $\hat{b}_1$, $\hat{b}_2$, and $\hat{b}_3$, indicated by arrows with crosses. From Fig. 1(a), we can see that both $\hat{a}_1$ and $\hat{a}_3$ ($\hat{a}_2$ and $\hat{a}_4$) act as idler (signal) beams. It is well known that the output beams of FWM processes in the same roles, i.e., idler and idler beams, as well as signal and signal beams, cannot entangle with each other as they have never interacted with each other directly [56]. It is the same reason as for the absence of steering among idler beams $\hat{b}_1$, $\hat{b}_2$, and $\hat{b}_3$.

Second, the states manifest asymmetric even "one-way" steering between different pairs in the two structures, as shown in Fig. 2. We plot in Fig. 8 all asymmetric steerings using green solid arrows for deterministic steering and dashed arrows for conditional steering. For example, in the asymmetric structure shown in Fig. 8(b), mode $\hat{b}_4$ can always steer the other three modes but can be steered by individual modes conditional on the values of the gain factors. The reason may be attributed to the asymmetrical influence of thermal noise on the steering in two directions. As shown in Fig. 1(e), the signal beam $\hat{b}_4$ comes from the continuously amplified seed input $\hat{a}_{s,0}$ by three FWM processes which generate thermal states by adding extra vacuum noise to the signal beam. To make it clear, let us analyze the steering between modes $\hat{b}_1$ and $\hat{b}_4$ as an example. After the FWM1 process, the two outputs $\hat{b}_1$ and $\hat{a}_{s1}$ are entangled with each other with symmetric steerability [see Eqs. (A2c) and (A2j) in Appendix 2, where $G_2 = G_3 = 1$, $\mathcal{G}^{b_1\to b_4} = \mathcal{G}^{b_4\to b_1}$]; then the beam $\hat{a}_{s1}$ goes through the second and third Rb vapor cells and becomes mode $\hat{b}_4$. Note that FWM2 and FWM3 act together on the signal beam $\hat{a}_{s1}$ to make it into a thermal state with thermal noises controlled by the gain factors G_2 and G_3. This destroys the steering between $\hat{b}_1$ and $\hat{b}_4$, and the larger G_2 and G_3 are, the smaller the steerability becomes. However, the effect of thermal noise on the steering in two directions is asymmetric; that is, the steering of $\hat{b}_1 \to \hat{b}_4$ is more sensitive to the effect of thermal noise and can be achieved only when $G_3^2 < (2G_1^2 - 1)/(G_1^2G_2^2)$, while the steering in the other direction $\hat{b}_4 \to \hat{b}_1$ cannot be fully destroyed by increasing thermal noise as mode $\hat{b}_1$ is not thermally excited [9,57]. With similar analysis, we can see that $\mathcal{G}^{b_2\to b_4} > 0$ when $G_3^2 < (2G_1^2G_2^2 - 2G_1^2 + 1)/(G_1^2G_2^2)$ and

$\mathcal{G}^{b_3\to b_4} > 0$ when $G_3^2 > (2G_1^2G_2^2 - 1)/(G_1^2G_2^2)$, while no such conditions exist for the steering in the opposite directions, i.e., $\mathcal{G}^{b_4\to b_2} > 0$ and $\mathcal{G}^{b_4\to b_3} > 0$ for all practical parameters [analytical solutions are given in Eqs. (A2k) and (A2l) in Appendix 2]. From the above conditions and ensuring $G_1, G_2, G_3 > 1$, we can also see that it is not possible to achieve the steering from individual modes $\hat{b}_1$, $\hat{b}_2$, and $\hat{b}_3$ to $\hat{b}_4$ simultaneously. Notice that although the pairwise steerability may decrease by cascading more FWM processes, the total quantum correlation of the system is enhanced, as evidenced by the increasing steerability of $\mathcal{G}^{b_1b_2b_3\to b_4}$ in Fig. 4(b).

The third difference in the states created by the two structures is that the value of G_2 does not affect the steerability $\mathcal{G}^{a_3\to a_4}$ produced by the symmetric FWM process but does affect the steerability $\mathcal{G}^{b_3\to b_4}$ created by the asymmetric case. This is because the FWM2 and FWM3 processes in the symmetric structure are independent events; adjusting G_2 (G_3) does not influence the steering between modes $\hat{a}_3$ and $\hat{a}_4$ ($\hat{a}_1$ and $\hat{a}_2$). Nevertheless, for the asymmetric structure, any gain of three FWM processes has an effect on the steerability. In Fig. 2(b), one can see that $\mathcal{G}^{b_4\to b_3}$ slightly grows when G_2 decreases from 2 to 1.2, as the noise effect caused by FWM2 is weakening.

B. Eigenmode of the four-mode Gaussian states

In Figs. 3 and 7 we observe the lifting of the constraint introduced by the type-II Gaussian monogamy relation for the symmetric cascaded FWM processes, where $\mathcal{G}^{a_2\to(a_1a_3)} > 0$ $\mathcal{G}^{a_4\to(a_1a_3)} > 0$, as indicated in Fig. 3(c), and $\mathcal{G}^{a_1\to(a_2a_4)} > 0$ $\mathcal{G}^{a_3\to(a_2a_4)} > 0$, as indicated in Fig. 7(a). It is not observed for the states created by the cascaded FWM processes in the asymmetric structure.

The first reason is that in the asymmetric structure, the quantum steering cannot be created among idler beams $\hat{b}_1$, $\hat{b}_2$, and $\hat{b}_3$; that is, we cannot get any steerability among them unless the signal mode $\hat{b}_4$ is involved. When mode $\hat{b}_4$ acts as a steering party, one cannot find any other signal mode that can act in the same role to steer the remaining modes. When mode $\hat{b}_4$ is one of the steered modes, we find that it is still impossible to realize $\mathcal{G}^{b_1\to(b_2b_4)} > 0$ and $\mathcal{G}^{b_3\to(b_2b_4)} > 0$ simultaneously. Because the symplectic eigenvalues of their corresponding Schur complements are reciprocal, only one of these two steerabilities can be greater than zero (other combinations are the same, as detailed in Appendix 3).

Second, our result also suggests that the lifting of the constraint may happen when more eigensqueezers coexist in the system. Using the Bloch-Messiah reduction, a multipartite Gaussian state can be decomposed into a unique set of uncorrelated single-mode squeezers and passive (linear) unitaries [48,49]. For instance, the correlations terms related to the amplitude quadrature X_i in the CM of a four-mode Gaussian state created by the symmetric structure, which is determined by Eq. (2a),

$$C_{X,sym} = \begin{pmatrix} 2G_1^2G_2^2 - 1 & 2g_2G_1^2G_2 & 2g_1g_3G_1G_2 & 2g_1G_1G_2G_3 \\ 2g_2G_1^2G_2 & 1 + 2G_1^2\left(G_2^2 - 1\right) & 2g_1g_2g_3G_1 & 2g_1g_2G_1G_3 \\ 2g_1g_3G_1G_2 & 2g_1g_2g_3G_1 & 1 + 2G_1^2\left(G_3^2 - 1\right) & 2g_3G_1^2G_3 \\ 2g_1G_1G_2G_3 & 2g_1g_2G_1G_3 & 2g_3G_1^2G_3 & 2G_1^2G_3^2 - 1 \end{pmatrix}, \tag{6}$$

can be diagonalized with eigenvalues 0.125, 0.436, 2.296, and 7.972 when $G_1 = G_2 = G_3 = 1.2$. Correspondingly, the momentum (phase) quadrature contains the same eigenmodes with inverse eigenvalues in the case of pure states. Based on the method introduced in Refs. [48,49], each eigenvalue represents the variance of an eigenmode for the amplitude quadrature. When one of these eigenvalues is larger (smaller) than 1 (vacuum mode), the system is composed of one squeezed (antisqueezed) mode in the amplitude quadrature. Therefore, the squeezing levels corresponding to those eigenvalues (variances) are −9.02, −3.61, 3.61, and 9.02 dB, as plotted in Figs. 9(a)–9(d). This means the output four-mode Gaussian states can be decomposed into four independent squeezers (two squeezed in the amplitude quadrature and two squeezed in the phase quadrature) with linear unitaries (e.g., a linear optical network composed by beam splitters).

Similarly, we transform the four-mode Gaussian states generated by the asymmetric structure into a set of uncorrelated squeezers and find there are only two squeezed eigenmodes with levels of squeezing: {−9.93, 0, 0, 9.93 dB}, as shown in Figs. 9(e)–9(h). The eigenmode components and squeezing levels change for different gain settings in both structures. It is clear that more squeezed eigenmodes may be generated by cascading more FWM processes in the symmetric structure, while cascading more FWM processes in the asymmetric case generates larger squeezing values but keeps only two squeezed eigenmodes. The total level of quantum correlations in the system is determined by the squeezing value of eigensqueezers, and thus, the collective steerability indicated by the residual Gaussian steering, stemming from the type-III and type-IV monogamy relations, in the asymmetric case is significantly stronger than that created in the symmetric setup, as shown in Figs. 4–7. In addition, more independent eigensqueezers existing in the symmetric structure may bring more abundant structures to the quantum steering in the system such as the lifting of the type-II monogamy constraint. What's more, compared with the multipartite entangled states generated by linear optics networks [27,28], from the above analysis, we can clearly see that by adjusting the structures of cascaded FWM processes, one can create entangled states with steering shared among different modes and can even enhance the total steerability involved in the system without changing the pump and gains. However, to realize this by linear optics networks

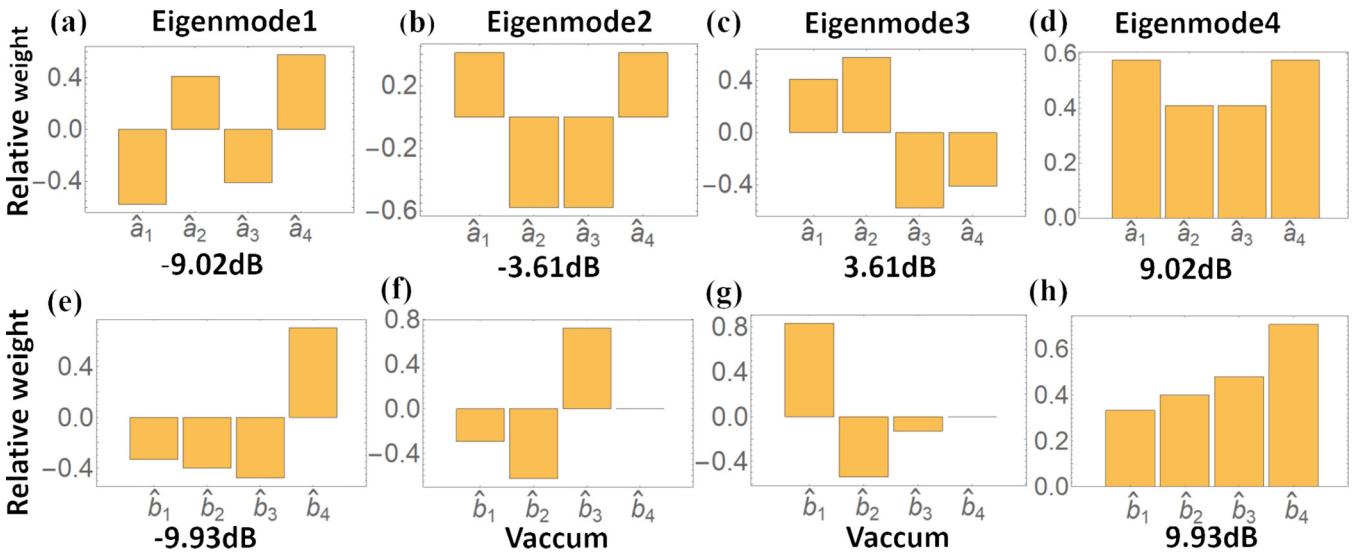

FIG. 9. Eigenmodes decomposed from the four-mode Gaussian states for two schemes with the same pump power. The bars in (a)–(d) and (e)–(h) represent the relative weight of modes $\hat{a}_{1,2,3,4}$ and $\hat{b}_{1,2,3,4}$, respectively. Eigenmodes 1 and 4, 2 and 3 have the same squeezing levels in the amplitude and phase quadratures, respectively.

[27,28], one has to change the squeezing inputs as well as the linear structure of the networks (the transformation unitary matrix).

V. SUMMARY

Different structures of cascaded FWM processes are useful for creating various multipartite entangled states that are abundant in multimode quantum steering and are useful for a variety of quantum communication tasks. For instance, in the region of $1.08 < G_3 < 1.14$ (with fixed $G_1 = G_2 = 1.2$) shown in Fig. 4(a), mode $\hat{a}_4$ can be steered by $(\hat{a}_1\hat{a}_2\hat{a}_3)$ together but cannot be steered by any individual mode ($\mathcal{G}^{a_1a_2a_3\to a_4} > 0$, $\mathcal{G}^{a_1\to a_4} = \mathcal{G}^{a_2\to a_4} = \mathcal{G}^{a_3\to a_4} = 0$). A similar property is observed in the asymmetric case when $1.04 < G_3 < 1.23$. This means that the values of amplitudes of $\hat{a}_4$ ($\hat{b}_4$) cannot be inferred to high precision by one mode alone and must be inferred collectively by a group. Therefore, the values of amplitudes of $\hat{a}_4$ can form the basis for a key which can be deciphered only by receivers $\hat{a}_1$, $\hat{a}_2$, $\hat{a}_3$ collaboratively with a low uncertainty. Unlike ordinary entanglement (state inseparability), the steering nonlocality cannot be faked by classical means assuming the station of mode $\hat{a}_4$ is secure (trusted), without the assumption of trust in the collaborating receivers' measurement devices [58]. The amount of residual steerability achieved in both schemes is, in principle, high enough to demonstrate secure continuous-variable 1sDI quantum secret sharing with nonzero key rates [24]; for example, the steerabilities are required to be larger than $\ln(e/2)$. Note that creating the same level of multimode steerability with linear optics networks [27,28] requires more effort to either improve the squeezing level of the input states or generate more single-mode squeezers.

In summary, we proposed two different schemes, i.e., the symmetric and asymmetric structures of three cascaded FWM processes in Rb atomic vapors, to generate four-mode Gaussian entangled states. We investigated the steering properties shared by two-, three-, and four-mode steering, which could be actively modulated by adjusting the gain values of FWM processes in both structures. By examining the monogamy relations for Gaussian steering, we found in the symmetric case that there is a lifting of the constraint given by the type-II monogamy relation when the steered party contains more than one mode. The steering properties, especially the asymmetric steering, and the lifting of the constraint were analyzed by considering the difference in the two structures and the independent squeezed eigenmodes decomposed from the four-mode Gaussian states. The present results help people to understand the distribution rules of multipartite steering in the FWM platform and pave the way to generate on-demand multipartite EPR steering for a quantum network.

ACKNOWLEDGMENTS

Y.X. acknowledges the National Postdoctoral Program for Innovative Talents (Grant No. BX20180015) and the China Postdoctoral Science Foundation (Grant No. 2019M650291). Y.C. and Y.L. recognize the National Natural Science Foundation of China (Grants No. 11904279, No. 61975159, and No. 11804267), the National Key R&D Program of China (Grants No. 2017YFA0303700), and the National Science Foundation of Jiangsu Province (Grant No. BK20180322). Q.H. thanks the National Natural Science Foundation of China (Grants No. 11622428, No. 11975026, and No. 61675007), the Beijing Natural Science Foundation (Grant No. Z190005), and the Key R&D Program of Guangdong Province (Grant No. 2018B030329001).

APPENDIX: SOLUTION TO (1 + 1)- AND (1 + 2)-MODE EPR STEERING

1. The solution to (1 + 1)-mode EPR steering of the symmetric structure ($G_1 > 1$, $G_2 > 1$, and $G_3 > 1$)

$$\mathcal{G}^{a_1\to a_2} = -\ln\left(1-\frac{2G_1^2(G_2^2-1)}{2G_1^2G_2^2-1}\right) > 0, \tag{A1a}$$

$$\mathcal{G}^{a_1\to a_3} = \max\left\{0, -\ln\left(\frac{2G_1^2(2G_2^2G_3^2-G_2^2-G_3^2+1)-1}{2G_1^2G_2^2-1}\right)\right\} = 0, \tag{A1b}$$

$$\mathcal{G}^{a_1\to a_4} = \max\left\{0, -\ln\left(\frac{2G_1^2G_3^2(2G_2^2-1)}{2G_1^2G_2^2-1}-1\right)\right\}, \tag{A1c}$$

$$\mathcal{G}^{a_2\to a_1} = \max\left\{0, -\ln\left(\frac{2G_1^2G_2^2}{2G_1^2(G_2^2-1)+1}-1\right)\right\}, \tag{A1d}$$

$$\mathcal{G}^{a_2\to a_3} = \max\left\{0, -\ln\left(\frac{2G_1^2(2G_2^2G_3^2-G_2^2-G_3^2)+1}{2G_1^2(G_2^2-1)+1}\right)\right\} = 0, \tag{A1e}$$

$$\mathcal{G}^{a_2\to a_4} = \max\left\{0, -\ln\left(\frac{2G_1^2(2G_2^2G_3^2-G_2^2-G_3^2+1)-1}{2G_1^2(G_2^2-1)+1}\right)\right\} = 0, \tag{A1f}$$

$$\mathcal{G}^{a_3\to a_1} = \max\left\{0, -\ln\left(\frac{2G_1^2(2G_2^2G_3^2-G_2^2-G_3^2+1)-1}{2G_1^2(G_3^2-1)+1}\right)\right\} = 0, \tag{A1g}$$

$$\mathcal{G}^{a_3\to a_2} = \max\left\{0, -\ln\left(\frac{2G_1^2(2G_2^2G_3^2-G_2^2-G_3^2)+1}{2G_1^2(G_3^2-1)+1}\right)\right\} = 0, \tag{A1h}$$

$$\mathcal{G}^{a_3\to a_4} = \max\left\{0, -\ln\left(\frac{2G_1^2G_3^2}{2G_1^2(G_3^2-1)+1}-1\right)\right\}, \tag{A1i}$$

$$\mathcal{G}^{a_4\to a_1} = \max\left\{0, -\ln\left(\frac{2G_1^2G_2^2(2G_3^2-1)}{2G_1^2G_3^2-1}-1\right)\right\}, \tag{A1j}$$

$$\mathcal{G}^{a_4\to a_2} = \max\left\{0, -\ln\left(\frac{2G_1^2(2G_2^2G_3^2-G_2^2-G_3^2+1)-1}{2G_1^2G_3^2-1}\right)\right\} = 0, \tag{A1k}$$

$$\mathcal{G}^{a_4\to a_3} = -\ln\left(1-\frac{2G_1^2(G_3^2-1)}{2G_1^2G_3^2-1}\right) > 0. \tag{A1l}$$

2. The solution to (1 + 1)-mode EPR steering of the asymmetric structure ($G_1 > 1$, $G_2 > 1$, and $G_3 > 1$)

$$\mathcal{G}^{b_1\to b_2} = \max\left\{0, -\ln\left(1+\frac{2G_1^2(G_2^2-1)}{2G_1^2-1}\right)\right\} = 0, \tag{A2a}$$

$$\mathcal{G}^{b_1\to b_3} = \max\left\{0, -\ln\left(1+\frac{2G_1^2G_2^2(G_3^2-1)}{2G_1^2-1}\right)\right\} = 0, \tag{A2b}$$

$$\mathcal{G}^{b_1\to b_4} = \max\left\{0, -\ln\left(\frac{2G_1^2G_2^2G_3^2}{2G_1^2-1}-1\right)\right\}, \tag{A2c}$$

$$\mathcal{G}^{b_2\to b_1} = \max\left\{0, -\ln\left(1+\frac{2(G_1^2-1)}{2G_1^2(G_2^2-1)+1}\right)\right\} = 0, \tag{A2d}$$

$$\mathcal{G}^{b_2\to b_3} = \max\left\{0, -\ln\left(1+\frac{2G_1^2G_2^2(G_3^2-1)}{2G_1^2G_2^2-2G_1^2+1}\right)\right\} = 0, \tag{A2e}$$

$$\mathcal{G}^{b_2\to b_4} = \max\left\{0, -\ln\left(\frac{2G_1^2G_2^2G_3^2}{2G_1^2(G_2^2-1)+1}-1\right)\right\}, \tag{A2f}$$

$$\mathcal{G}^{b_3\to b_1} = \max\left\{0, -\ln\left(1+\frac{2(G_1^2-1)}{2G_1^2G_2^2G_3^2-2G_1^2G_2^2+1}\right)\right\} = 0, \tag{A2g}$$

$$\mathcal{G}^{b_3\to b_2} = \max\left\{0, -\ln\left(1+\frac{2G_1^2(G_2^2-1)}{2G_1^2G_2^2G_3^2-2G_1^2G_2^2+1}\right)\right\} = 0, \tag{A2h}$$

$$\mathcal{G}^{b_3\to b_4} = \max\left\{0, -\ln\left(\frac{2G_1^2G_2^2G_3^2}{2G_1^2G_2^2(G_3^2-1)+1}-1\right)\right\}, \tag{A2i}$$

$$\mathcal{G}^{b_4\to b_1} = -\ln\left(1-\frac{2(G_1^2-1)}{2G_1^2G_2^2G_3^2-1}\right) > 0, \tag{A2j}$$

$$\mathcal{G}^{b_4\to b_2} = -\ln\left(1-\frac{2G_1^2(G_2^2-1)}{2G_1^2G_2^2G_3^2-1}\right) > 0, \tag{A2k}$$

$$\mathcal{G}^{b_4\to b_3} = -\ln\left(1-\frac{2G_1^2G_2^2(G_3^2-1)}{2G_1^2G_2^2G_3^2-1}\right) > 0. \tag{A2l}$$

3. The solution to (1 + 2)-mode EPR steering of the asymmetric structure ($G_1 > 1$, $G_2 > 1$, and $G_3 > 1$)

$$\mathcal{G}^{b_2\to(b_1b_4)} = \max\left\{0, -\ln\left(\frac{2G_1^2G_2^2G_3^2-2G_1^2G_2^2+1}{2G_1^2G_2^2-2G_1^2+1}\right)\right\}, \tag{A3a}$$

$$\mathcal{G}^{b_3\to(b_1b_4)} = \max\left\{0, -\ln\left(\frac{2G_1^2G_2^2-2G_1^2+1}{2G_1^2G_2^2G_3^2-2G_1^2G_2^2+1}\right)\right\}, \tag{A3b}$$

$$\mathcal{G}^{b_1\to(b_2b_4)} = \max\left\{0, -\ln\left(\frac{2G_1^2G_2^2G_3^2-2G_1^2G_2^2+1}{2G_1^2-1}\right)\right\}, \tag{A3c}$$

$$\mathcal{G}^{b_3\to(b_2b_4)} = \max\left\{0, -\ln\left(\frac{2G_1^2-1}{2G_1^2G_2^2G_3^2-2G_1^2G_2^2+1}\right)\right\}, \tag{A3d}$$

$$\mathcal{G}^{b_1\to(b_3b_4)} = \max\left\{0, -\ln\left(\frac{2G_1^2G_2^2-2G_1^2+1}{2G_1^2-1}\right)\right\}, \tag{A3e}$$

$$\mathcal{G}^{b_2\to(b_3b_4)} = \max\left\{0, -\ln\left(\frac{2G_1^2-1}{2G_1^2G_2^2-2G_1^2+1}\right)\right\}. \tag{A3f}$$

[1] E. Schrödinger, Proc. Cambridge Philos. Soc. **31**, 555 (1935).
[2] A. Einstein, B. Podolsky, and N. Rosen, Phys. Rev. **47**, 777 (1935).
[3] M. D. Reid, Phys. Rev. A **40**, 913 (1989).
[4] H. M. Wiseman, S. J. Jones, and A. C. Doherty, Phys. Rev. Lett. **98**, 140402 (2007).
[5] S. J. Jones, H. M. Wiseman, and A. C. Doherty, Phys. Rev. A **76**, 052116 (2007).
[6] M. D. Reid, P. D. Drummond, W. P. Bowen, E. G. Cavalcanti, P. K. Lam, H. A. Bachor, U. L. Andersen, and G. Leuchs, Rev. Mod. Phys. **81**, 1727 (2009).
[7] E. G. Cavalcanti, S. J. Jones, H. M. Wiseman, and M. D. Reid, Phys. Rev. A **80**, 032112 (2009).
[8] J. Bowles, T. Vértesi, M. T. Quintino, and N. Brunner, Phys. Rev. Lett. **112**, 200402 (2014).
[9] Q. Y. He, Q. H. Gong, and M. D. Reid, Phys. Rev. Lett. **114**, 060402 (2015).
[10] V. Händchen, T. Eberle, S. Steinlechner, A. Samblowski, T. Franz, R. F. Werner, and R. Schnabel, Nat. Photonics **6**, 596 (2012).
[11] S. Wollmann, N. Walk, A. J. Bennet, H. M. Wiseman, and G. J. Pryde, Phys. Rev. Lett. **116**, 160403 (2016).
[12] K. Sun, X.-J. Ye, J.-S. Xu, X.-Y. Xu, J.-S. Tang, Y.-C. Wu, J.-L. Chen, C.-F. Li, and G.-C. Guo, Phys. Rev. Lett. **116**, 160404 (2016).

[13] C. Branciard, E. G. Cavalcanti, S. P. Walborn, V. Scarani, and H. M. Wiseman, Phys. Rev. A **85**, 010301(R) (2012).

[14] N. Walk, S. Hosseini, J. Geng, O. Thearle, J. Y. Haw, S. Armstrong, S. M. Assad, J. Janousek, T. C. Ralph, T. Symul *et al.*, Optica **3**, 634 (2016).

[15] I. Kogias, Y. Xiang, Q. He, and G. Adesso, Phys. Rev. A **95**, 012315 (2017).

[16] M. D. Reid, Phys. Rev. A **88**, 062338 (2013).

[17] Q. Y. He, L. Rosales-Zárate, G. Adesso, and M. D. Reid, Phys. Rev. Lett. **115**, 180502 (2015).

[18] C.-Y. Chiu, N. Lambert, T.-L. Liao, F. Nori, and C.-M. Li, npj Quantum Inf. **2**, 16020 (2016).

[19] M. Piani and J. Watrous, Phys. Rev. Lett. **114**, 060404 (2015).

[20] R. Uola, A. C. S. Costa, H. C. Nguyen, and O. Gühne, Rev. Mod. Phys. **92**, 015001 (2020).

[21] Q. Y. He and M. D. Reid, Phys. Rev. Lett. **111**, 250403 (2013).

[22] I. Kogias, A. R. Lee, S. Ragy, and G. Adesso, Phys. Rev. Lett. **114**, 060403 (2015).

[23] A. Riccardi, C. Macchiavello, and L. Maccone, Phys. Rev. A **97**, 052307 (2018).

[24] Y. Xiang, I. Kogias, G. Adesso, and Q. He, Phys. Rev. A **95**, 010101(R) (2017).

[25] M. Wang, Q. Gong, and Q. He, Opt. Lett. **39**, 6703 (2014).

[26] D. Cavalcanti, P. Skrzypczyk, G. H. Aguilar, R. V. Nery, P. H. Ribeiro, and S. P. Walborn, Nat. Commun. **6**, 7941 (2015).

[27] X. Deng, Y. Xiang, C. Tian, G. Adesso, Q. He, Q. Gong, X. Su, C. Xie, and K. Peng, Phys. Rev. Lett. **118**, 230501 (2017).

[28] S. Armstrong, W. Meng, R. Y. Teh, Q. Gong, Q. He, J. Janousek, H. A. Bachor, M. D. Reid, and K. L. Ping, Nat. Phys. **11**, 167 (2015).

[29] Y. Cai, Y. Xiang, Y. Liu, Q. He, and N. Treps, arXiv:1910.13698.

[30] C. F. Mccormick, V. Boyer, E. Arimondo, and P. D. Lett, Opt. Lett. **32**, 178 (2007).

[31] J. Du, L. Cao, K. Zhang, and J. Jing, Appl. Phys. Lett. **110**, 241103 (2017).

[32] L. Wang, S. Lv, and J. Jing, Opt. Express **25**, 17457 (2017).

[33] Z. Qin, L. Cao, H. Wang, A. M. Marino, W. Zhang, and J. Jing, Phys. Rev. Lett. **113**, 023602 (2014).

[34] L. Cao, J. Qi, J. Du, and J. Jing, Phys. Rev. A **95**, 023803 (2017).

[35] Z. Qin, L. Cao, and J. Jing, Appl. Phys. Lett. **106**, 211104 (2015).

[36] S. Lv and J. Jing, Phys. Rev. A **96**, 043873 (2017).

[37] V. Boyer, A. M. Marino, and P. D. Lett, Phys. Rev. Lett. **100**, 143601 (2008).

[38] X. Pan, S. Yu, Y. Zhou, K. Zhang, K. Zhang, S. Lv, S. Li, W. Wang, and J. Jing, Phys. Rev. Lett. **123**, 070506 (2019).

[39] D.-S. Ding, W. Zhang, Z.-Y. Zhou, S. Shi, B.-S. Shi, and G.-C. Guo, Nat. Photonics **9**, 332 (2015).

[40] C. Shu, X. Guo, P. Chen, M. M. T. Loy, and S. Du, Phys. Rev. A **91**, 043820 (2015).

[41] Y. Wang, J. Li, S. Zhang, K. Su, Y. Zhou, K. Liao, S. Du, H. Yan, and S.-L. Zhu, Nat. Photonics **13**, 346 (2019).

[42] A. M. Marino, R. C. Pooser, V. Boyer, and P. D. Lett, Nature (London) **457**, 859 (2009).

[43] J. Jing, C. Liu, Z. Zhou, Z. Y. Ou, and W. Zhang, Appl. Phys. Lett. **99**, 011110 (2011).

[44] Z. Y. Ou, Phys. Rev. A **85**, 023815 (2012).

[45] F. Hudelist, J. Kong, C. Liu, J. Jing, Z. Y. Ou, and W. Zhang, Nat. Commun. **5**, 3049 (2014).

[46] Y. Cai, J. Feng, H. Wang, G. Ferrini, X. Xu, J. Jing, and N. Treps, Phys. Rev. A **91**, 013843 (2015).

[47] A. MacRae, T. Brannan, R. Achal, and A. I. Lvovsky, Phys. Rev. Lett. **109**, 033601 (2012).

[48] S. L. Braunstein, Phys. Rev. A **71**, 055801 (2005).

[49] Y. Cai, J. Roslund, G. Ferrini, F. Arzani, X. Xu, C. Fabre, and N. Treps, Nat. Commun. **8**, 15645 (2017).

[50] D. Zhang, C. Li, Z. Zhang, Y. Zhang, Y. Zhang, and M. Xiao, Phys. Rev. A **96**, 043847 (2017).

[51] Y. Xiang, B. Xu, L. Mišta, T. Tufarelli, Q. He, and G. Adesso, Phys. Rev. A **96**, 042326 (2017).

[52] M. D. Reid, Phys. Rev. A **88**, 062108 (2013).

[53] S.-W. Ji, M. S. Kim, and H. Nha, J. Phys. A **48**, 135301 (2015).

[54] G. Adesso and R. Simon, J. Phys. A **49**, 34LT02 (2016).

[55] L. Lami, C. Hirche, G. Adesso, and A. Winter, Phys. Rev. Lett. **117**, 220502 (2016).

[56] M. Jasperse, L. D. Turner, and R. E. Scholten, Opt. Express **19**, 3765 (2011).

[57] Q. Y. He and M. D. Reid, Phys. Rev. A **88**, 052121 (2013).

[58] B. Opanchuk, L. Arnaud, and M. D. Reid, Phys. Rev. A **89**, 062101 (2014).